

## Article

# Tide Prediction in the Venice Lagoon Using Nonlinear Autoregressive Exogenous (NARX) Neural Network

Fabio Di Nunno , Giovanni de Marinis , Rudy Gargano  and Francesco Granata \* 

Department of Civil and Mechanical Engineering (DICEM), University of Cassino and Southern Lazio, Via Di Biasio, 43, 03043 Cassino, Frosinone, Italy; fabio.dinunno@unicas.it (F.D.N.); demarinis@unicas.it (G.d.M.); gargano@unicas.it (R.G.)

\* Correspondence: f.granata@unicas.it

**Abstract:** In the Venice Lagoon some of the highest tides in the Mediterranean occur, which have influenced the evolution of the city of Venice and the surrounding lagoon for centuries. The forecast of “high waters” in the lagoon has always been a matter of considerable practical interest. In this study, tide prediction models were developed for the entire lagoon based on Nonlinear Autoregressive Exogenous (NARX) neural networks. The NARX-based model development was performed in two different stages. The first stage was the training and testing of the NARX network, performed on data collected in a given time interval at the tide gauge of Punta della Salute, at the end of Canal Grande. The second stage consisted of a comprehensive validation of the model in the entire Venice Lagoon, with a detailed analysis of data from three measuring stations located in points of the lagoon with different characteristics. Good predictions were achieved regardless of whether the meteorological parameters were considered among input parameters, even with considerable time advance. Furthermore, the forecasting model based on NARX has proved capable of predicting even exceptional high tides. The proposed model could be a useful support tool for the management of the MOSE system, which will protect Venice from high waters.



**Citation:** Di Nunno, F.; de Marinis, G.; Gargano, R.; Granata, F. Tide Prediction in the Venice Lagoon Using Nonlinear Autoregressive Exogenous (NARX) Neural Network. *Water* **2021**, *13*, 1173. <https://doi.org/10.3390/w13091173>

Academic Editor: Zacharias Frontistis

Received: 3 April 2021  
Accepted: 22 April 2021  
Published: 24 April 2021

**Publisher's Note:** MDPI stays neutral with regard to jurisdictional claims in published maps and institutional affiliations.



**Copyright:** © 2021 by the authors. Licensee MDPI, Basel, Switzerland. This article is an open access article distributed under the terms and conditions of the Creative Commons Attribution (CC BY) license (<https://creativecommons.org/licenses/by/4.0/>).

**Keywords:** tide prediction; artificial neural network; NARX; Venice Lagoon

## 1. Introduction

The city of Venice is a UNESCO world heritage site for the uniqueness of its historical, archaeological, urban, architectural, and artistic legacy. The historic center of Venice is located in the middle of the Venice Lagoon, a closed bay at the northwestern end of the Adriatic Sea. In this area, some of the highest tides in the Mediterranean occur [1]. Over the centuries, high tides have caused significant damage to the city, threatening its cultural heritage [2]. The most relevant high tide events, called “acqua alta” (high waters) in Italian, have significantly influenced the socioeconomic and environmental aspects of the Venice Lagoon throughout history.

High-water events occur in the Lagoon when the effects of the astronomical tide due to the attraction of celestial bodies are enhanced by meteorological disturbances. The most relevant weather factors affecting the tide-level fluctuations are barometric pressure and the wind. In particular, the Scirocco wind, from the southeast, and the Bora wind, from north-northeast, can lead to significant increases compared to the normal astronomical oscillations of the tide level.

One of the first reliable measures of high tide in the Venice Lagoon dates back to 1848 when the water surface reached 140 cm above the mean sea level. This is an exceptional value considering that, currently, the average ground level of Venice is only 80 cm above the mean sea level. Indeed, during the 20th century, Venice lost 25 cm in ground level, approximately 15 cm because of subsidence mainly due to groundwater pumping in the nearby industrial area and about 10 cm due to eustatism [3]. The highest extreme observed event dates back to 4 November 1966, when the water level reached 194 cm [4]. More

recently, the second-highest tide occurred: a sea level equal to 187 cm was measured on 12 November 2019. The issue becomes more evident by observing that 15 exceptional events, with water level above 140 cm, have occurred in the past 20 years, while only 10 exceptional events had occurred in the previous 80 years [5]. In order to safeguard Venice and its lagoon from high waters, the MOSE (MODulo Sperimentale Elettromeccanico—Experimental Electromechanical Module) system is nearing completion. It consists of a submerged-barriers system that, in the case of tides higher than 110 cm, will rise, blocking the water fluxes from the Adriatic Sea [6]. However, the rising of the sea level still remains an open question on which it will be necessary to evaluate and possibly update the high-tides protection systems.

Therefore, an accurate prediction of the tide level in Venice is an issue of relevant practical and scientific interest. In literature, there are different approaches to forecast the tide level in the Venice Lagoon: statistical models, such as the BIGSUMDP expert model [7], hydrodynamic models [8,9], e.g., SHYFEM [10] and HYPSE [11,12] models, Support Vector Machine [13], linear autoregressive models [14], and nonlinear models, based on the cardinal B-spline (CBS) functions [15]. However, the results achieved with Support Vector Machine, linear autoregressive models and nonlinear models were accurate for a lag time between input data and forecast horizon lower than 24 h, while the statistical and hydrodynamic models require a large number of input data, making them complex to use. In the past few decades, Artificial Intelligence (AI) models have taken hold for the prediction of complex natural phenomena [16–22]. However, to date their application for the tide forecasting leads to accurate predictions only for a short forecast horizon [23] or is related to ocean environments with a reduced number of measurement points [24,25].

In general, the disadvantages of machine learning algorithms, such as Support Vector Machine, are related to relevant structure and computational complexities [26], which lead to long training times [27] and to the requirement of large datasets in order to properly evaluate the several algorithm parameters during the training stage [28].

Otherwise, autoregressive models with exogenous inputs, both linear (ARX) and nonlinear (NARX), allow, in comparison with different machine learning algorithms, an easier physical interpretation of the investigated parameter, based on the relationship between exogenous inputs and the target parameter. At the same time, the recursive update of predictors and model parameters allows for obtaining accurate forecasts even for short time series [29,30]. The aim of this study is the development of a novel prediction model of the tide in the entire Venetian lagoon, based on the Nonlinear Autoregressive Exogenous (NARX) neural networks, with a forecast horizon up to 72 h. NARX networks combine the Artificial Neural Networks (ANNs) with ARX models, allowing capture of the nonlinear behavior in an autoregressive time series [31].

The NARX approach proved to be particularly effective in modeling wave height [32] and groundwater level [33,34] time series. First, the NARX network was trained and tested with the tide-level data measured in Punta della Salute station, located near the historic center of Venice. Then, the trained network was used for a comprehensive modeling of the tide level in the Venice Lagoon, with a detailed analysis of three stations located in points of the lagoon with different characteristics relating to the propagation of the tide. Furthermore, the sensitivity of the performance to changes in the input variables and lag times was evaluated. A further detailed analysis was carried out on the most interesting aspect in tide modeling, which is represented by the prediction of exceptionally high tides. The proposed model could be a support tool for the decisions regarding the timely activation of the MOSE system in the Venice lagoon. Indeed, the setting of the MOSE barriers needs 48 h; therefore, reliable forecasting of the tides—with a predictive horizon up to 72 h—is a fundamental need to protect Venice. Some recent extreme events of the tide in the Venice Lagoon showed the necessity to improve the forecasting models. In fact, inaccurate forecasting did not allow the activation of the MOSE barriers, and Venice was again flooded.

## 2. Materials and Methods

### 2.1. Study Area and Dataset

The Venice Lagoon extends for 550 km<sup>2</sup> from the Sile River in the north to the Brenta River in the south, making the Venice Lagoon the largest wetland in the Mediterranean Basin [35,36]. For 80% of its surface, it consists of mudflats, tidal shallows, and salt marshes. About 11% is permanently covered by open water, while only 8% is represented by land, including the city of Venice and many smaller islands. The lagoon is connected to the Adriatic Sea by means of three inlets: Lido, Malamocco, and Chioggia.

The tide-level dataset consisted of measures on a network of 19 tide-gauge stations covering the Venice Lagoon. Wind direction, wind speed, and barometric pressure were taken from a weather station, referred to as Piattaforma CNR and located in the Adriatic Sea 13 km from the Malamocco inlet. For each station, data measured every 30 min were available and were used in the analysis.

Both the time series of the tide-gauge station Punta della Salute and the time series of the weather station were available for the period from January 2009 to December 2014. In addition, the gravitational effects were included in the prediction model by means of the astronomical tide height  $h_{astr}$ , which was computed through a harmonic analysis:

$$h_{astr} = A_0 + \sum_{n=1}^N A_n \cos(\sigma_n t - k_n) \quad (1)$$

where  $A_0$  is the average sea level,  $A_n$  is the amplitude,  $\sigma_n$  the angular frequency,  $k_n$  the phase delay of component  $n$ , and  $N$  is the number of harmonics used to evaluate the astronomical tide height. These values can be found on the Venice Municipality website [37]. Figure 1 shows the location of the tide gauge stations in the Venice Lagoon, and the weather station.

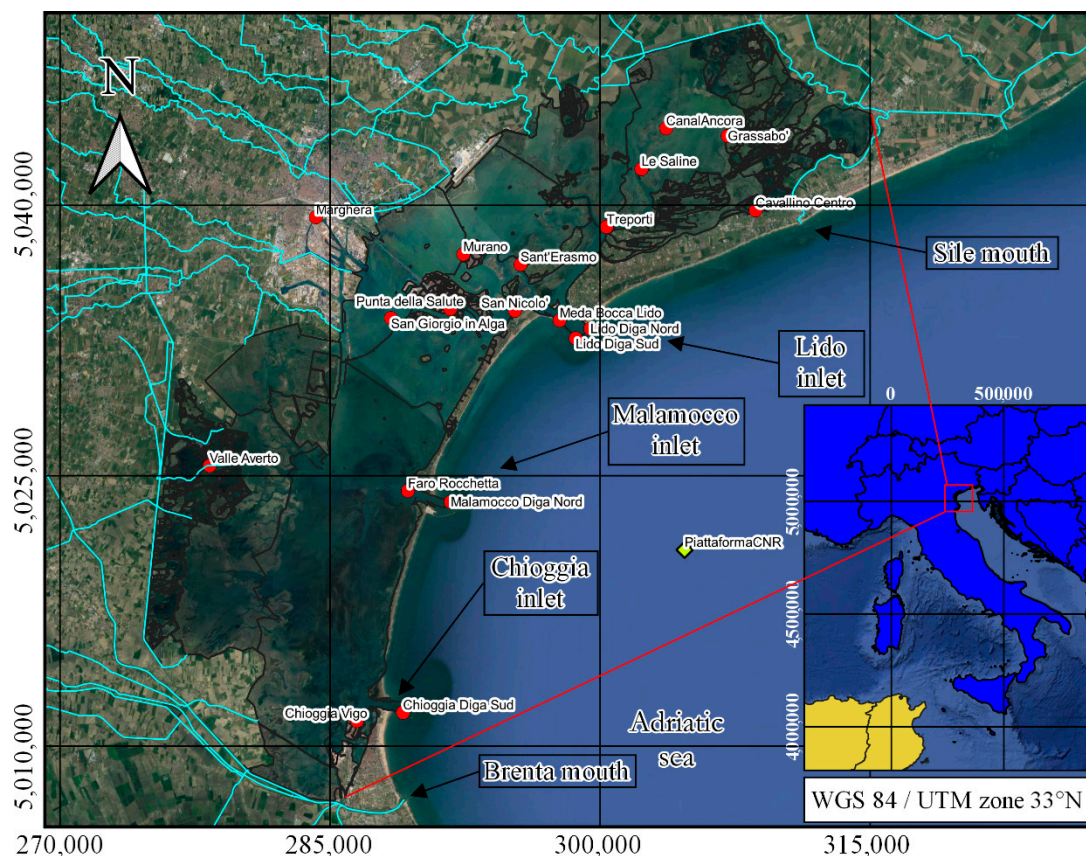


**Figure 1.** Location of the tide gauge (●) and weather station (◆), with a representation of the water-drainage network (–) on a satellite image of the Venice Lagoon.

## 2.2. NARX Model Architectures

NARX neural networks are a recurrent dynamic type of ANNs networks, which are composed of interconnected nodes inspired by a simplification of the biological neural system. Therefore, each node represents an artificial neuron that receives one or more inputs and sums them to produce an output. These sums pass through a function, known as an activation function, which, for the NARX network, is nonlinear. Based on the flow and processing information direction, different categories of ANNs can be distinguished. While in the feedforward neural networks (FNNs), the information flows in one direction with nodes arranged in layers; in the recurrent neural networks, such as NARX, information flows both in forward and backward directions, allowing a connection between neurons located in the same or previous layers [38]. The faster convergence in reaching the optimal connection weights between inputs and neurons and the reduced number of the latter to calibrate and make the model effective [39] makes NARX more high-performing compared to other ANNs and better at discovering long-time dependences in comparison with other recurrent neural networks [40]. Moreover, the exogenous inputs of the NARX network allow relating the current value of a time series to both past values of the same series and current and past values of the exogenous series, which represent the external series that affect the time series of interest. The basic equation for the NARX model is:

$$y(t) = f(y(t-1), y(t-2), \dots, y(t-n_y), u(t-1), u(t-2), \dots, u(t-n_u)) \quad (2)$$

where  $u(t)$  and  $y(t)$  are the input and output values at time  $t$ ,  $n_u$  and  $n_y$  are the input and output network layers, and  $f$  is the nonlinear function, approximated by the FNN.

The NARX architectures include 3 different and sequential layers (Figure 2). The first is the input layer, which consists of the input parameters of the neural network. The second is the hidden layer, which represents the computational step between input and output. The third is the output layer, which leads to the predicted value  $y(t)$ . Four different NARX-based models were implemented in MATLAB<sup>®</sup>2020a [41] environment. In all four models, both the lagged values of the tide level  $h_{tide}(t-t_a)$  and astronomical tide  $h_{astr}(t-t_a)$  were considered as input values while the output was represented by the predicted  $h_{tide}(t)$ , with  $t_a$  that is the lag time between input and target values. For each model, different combinations of additional input values were considered.

In the first model, indicated as “Model I”, the lagged wind speed  $v_{wind}(t-t_a)$ , the lagged wind direction  $\alpha_{wind}(t-t_a)$ , and the lagged barometric pressure  $P_{atm}(t-t_a)$ , were also considered as input values. In the second model, “Model II”,  $v_{wind}(t-t_a)$  and  $\alpha_{wind}(t-t_a)$  were considered as additional input values while for “Model III” only  $P_{atm}(t-t_a)$  was included as an additional input value. The fourth model, “Model IV”, did not have additional input values, taking into account only the lagged values of the tide level  $h_{tide}(t-t_a)$  and astronomical tide  $h_{astr}(t-t_a)$ . Therefore, input data were ahead of the tide value to be predicted for a time equal to the lag time  $t_a$ . It should be noted that, despite the fact that meteorological parameters were partly neglected, as for “Model II” and “Model III”, or completely neglected, as for “Model IV”, their influence is implicitly expressed by including previously observed tidal height values, which in turn also depend on meteorological factors. Moreover, as demonstrated by Di Nunno et al. (2021), considering only the lagged tide level  $h_{tide}(t-t_a)$  as an input variable led to relevant underestimation of the high tides. This made the astronomical tide an essential parameter for tide prediction [42].

Different lag time  $t_a$  values were considered, in order to assess the performance of the models as  $t_a$  increases. A preliminary analysis was conducted to select the optimal number of hidden nodes. The best performances were achieved for 3 hidden nodes (indicated in Figure 2 as  $h_1$ ,  $h_2$ , and  $h_3$ ). For the hidden layer, a sigmoid activation function  $f_1$  was used, while a linear activation function  $f_2$ , with only one neuron  $n$ , was used for the output layer. For the output layer (Figure 2), the weight  $w$  and bias  $b$  of the NARX model were optimized through the training algorithm described below.

The output value, represented by the predicted  $h_{tide}$ , was then fed back to the input values as part of the NARX architectures. In particular, the time delay  $t_a$  and the related

feedback delay, which is equal to the number of output values that were fed back as input, were both set to 1. This allowed minimizing the weight of fed-back values in the tide prediction.

The Bayesian Regularization was used as a training algorithm. It consists of a Gauss–Newton approximation to the Hessian matrix  $J^T(w)J(w)$ , where  $w$  is the weight vector,  $J$  is the Jacobian matrix, and  $J^T$  the transpose, based on the Bayesian technique [43], and implemented in the Levenberg–Marquardt algorithm, in order to reduce the probability of overfitting and the computational overhead [44]. The Levenberg–Marquardt algorithm approximates the Hessian matrix according to the equation [45]:

$$\Delta w = [J^T(w)J(w) + \lambda I]^{-1} J^T(w)e(w) \tag{3}$$

where  $I$  is the identity matrix,  $e$  is the error vector and  $\lambda$  is the learning constant, adjusted iteratively to find the minimum error. Despite a slow convergence with respect to the direct application of the Levenberg–Marquardt algorithm, the Bayesian Regularization algorithm usually leads to improved predictions [33].

Furthermore, a normalization of the input values was conducted in order to have a common range between 0 and 1 and improve the modeling performance. The tide level, the astronomical tide, the barometric pressure and the wind speed were normalized with respect to the respectively maximum values along the time series, while the wind direction was divided by 360:

$$h_{tide,i}^* = \frac{h_{tide,i}}{\max(h_{tide})} \tag{4}$$

$$h_{astr,i}^* = \frac{h_{astr,i}}{\max(h_{astr})} \tag{5}$$

$$P_{atm,i}^* = \frac{P_{atm,i}}{\max(P_{atm})} \tag{6}$$

$$v_{wind,i}^* = \frac{v_{wind,i}}{\max(v_{wind})} \tag{7}$$

$$\alpha_{wind,i}^* = \frac{\alpha_{wind,i}}{360} \tag{8}$$

where  $i$  indicates the temporal step.

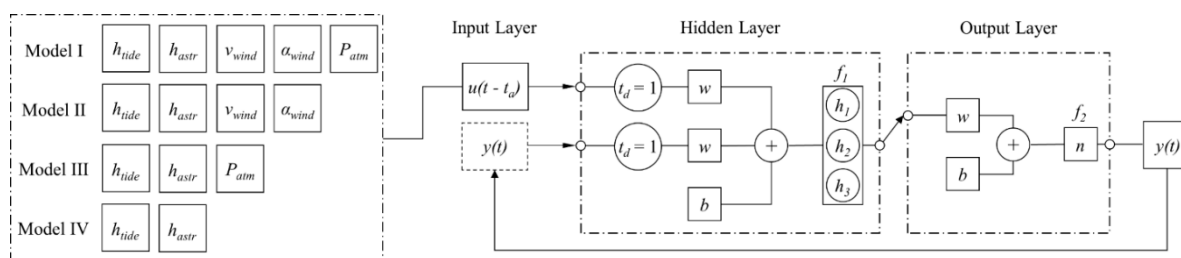


Figure 2. Sketch of the NARX model architecture.

### 2.3. Evaluation Metrics

The performance of the NARX network was evaluated by means of four evaluation metrics: the coefficient of determination  $R^2$ , which provides a measure of how well experimental data are replicated by the model, the Mean Absolute Error (MAE), which provides the average error magnitude for the predicted values, the Root Mean Squared Error (RMSE), which provides the square root of the average squared errors for the predicted values, and the Relative Absolute Error (RAE), which is the ratio between the absolute error and the

absolute value of the difference between average and each measured values. These metrics are defined as:

$$R^2 = 1 - \frac{\sum_{i=1}^m (f_i - y_i)^2}{\sum_{i=1}^m (y_a - y_i)^2} \quad (9)$$

$$MAE = \frac{\sum_{i=1}^m |f_i - y_i|}{m} \quad (10)$$

$$RMSE = \sqrt{\frac{\sum_{i=1}^m (f_i - y_i)^2}{m}} \quad (11)$$

$$RAE = \frac{\sum_{i=1}^m |f_i - y_i|}{\sum_{i=1}^m |y_a - y_i|} \quad (12)$$

where  $m$  is the total number of measured data,  $f_i$  is the predicted value for the  $i$ -th data,  $y_i$  is the experimental value for the  $i$ -th data, and  $y_a$  is the averaged value of the measured data.

### 3. Results and Discussion

The NARX modeling was performed in two different stages. The first was the training and testing of the NARX network-based model, performed for the period between January 2009 and December 2011 using the tide level dataset of Punta della Salute and the weather data of Piattaforma CNR. It should be noted that, for an accurate tide-level forecast, a time-series length of at least 12 months is required [42]. The second stage was an analysis extended to the Venice Lagoon, which consisted of validation of the NARX network for the tide prediction in the different tide gauge stations that cover the entire lagoon, including Punta della Salute. Validation was performed for periods not exceeding 1 year and not considered for the previous training and testing step, between January 2012 and December 2014. Table 1 reports, for each tide gauge station, the year considered for the model validation.

**Table 1.** Year considered for the tide prediction for each tide gauge station.

Tide Gauge Station	Year
Lido Diga Nord, Meda Bocca Lido, San Giorgio in Alga, Sant'Erasmus	2012
Canal Ancora, Chioggia Vigo, Faro Rocchetta, Grassabò, Le Saline, Malamocco Diga Nord, Marghera, Punta della Salute	2013
Chioggia Diga Sud, Cavallino Centro, Lido Diga Sud, Murano, San Nicolò, Treporti, Valle Averte	2014

#### 3.1. Training and Testing

With reference to the training and testing phases conducted on the data collected at the Punta della Salute tide gauge, the NARX-based model shows very good performance for all lag time and models (Table 2). The best performance was achieved for the lowest  $t_a$ , equal to 1 h, and Model I ( $R^2 = 0.9980 - RAE = 0.0426$ ). However, also for Model IV, which did not include the meteorological parameters among the input variables, the prediction was still very accurate, showing negligible differences compared to the other models ( $R^2 = 0.9980 - RAE = 0.0433$ ). For  $t_a = 2$  h (Model I— $R^2 = 0.9980 - RAE = 0.0437$ , Model IV— $R^2 = 0.9979 - RAE = 0.0443$ ), performances were slightly lower than those achieved for  $t_a = 1$  h.

**Table 2.** Prediction performance in the training and testing of the NARX network for the four models.

$t_a$ (Hours)	Model I				Model II				Model III				Model IV			
	$R^2$	MAE (cm)	RMSE (cm)	RAE	$R^2$	MAE (cm)	RMSE (cm)	RAE	$R^2$	MAE (cm)	RMSE (cm)	RAE	$R^2$	MAE (cm)	RMSE (cm)	RAE
1	0.9980	0.9668	1.2400	0.0426	0.9980	0.9773	1.2523	0.0431	0.9980	0.9797	1.2550	0.0432	0.9980	0.9831	1.2592	0.0433
2	0.9980	0.9929	1.2694	0.0437	0.9979	1.0160	1.2986	0.0448	0.9979	1.0136	1.2924	0.0447	0.9979	1.0058	1.2881	0.0443
3	0.9949	1.5830	1.9961	0.0697	0.9946	1.6305	2.0520	0.0718	0.9949	1.6015	2.0110	0.0705	0.9947	1.6272	2.0423	0.0717
6	0.9737	3.7215	4.5463	0.1639	0.9724	3.8238	4.6570	0.1684	0.9737	3.7246	4.5441	0.1640	0.9729	3.7752	4.6171	0.1662
12	0.9810	3.1069	3.8658	0.1368	0.9800	3.2172	3.9617	0.1417	0.9809	3.1123	3.8717	0.1371	0.9806	3.1506	3.9103	0.1388
18	0.9776	3.4265	4.2017	0.1509	0.9766	3.5183	4.2865	0.1549	0.9778	3.4101	4.1783	0.1502	0.9763	3.5566	4.3146	0.1566
24	0.9849	2.7610	3.4449	0.1216	0.9824	2.9933	3.7229	0.1318	0.9848	2.7622	3.4543	0.1216	0.9826	2.9653	3.6934	0.1306
30	0.9853	2.7086	3.4026	0.1193	0.9844	2.8079	3.4981	0.1236	0.9852	2.7156	3.4127	0.1196	0.9850	2.7444	3.4390	0.1208
36	0.9755	3.5943	4.3926	0.1582	0.9746	3.6599	4.4663	0.1611	0.9754	3.5982	4.3994	0.1584	0.9746	3.6486	4.4711	0.1606
42	0.9756	3.6013	4.3779	0.1585	0.9749	3.6765	4.4452	0.1618	0.9755	3.6065	4.3864	0.1587	0.9749	3.6762	4.4461	0.1618
48	0.9856	2.7151	3.3660	0.1195	0.9845	2.8283	3.4969	0.1245	0.9855	2.7229	3.3732	0.1199	0.9843	2.8414	3.5123	0.1251
54	0.9871	2.5676	3.1914	0.1130	0.9868	2.5922	3.2171	0.1141	0.9870	2.5700	3.1945	0.1131	0.9868	2.5953	3.2208	0.1142
60	0.9756	3.5952	4.3836	0.1582	0.9756	3.6023	4.3819	0.1585	0.9758	3.5764	4.3601	0.1574	0.9754	3.6060	4.3988	0.1587
66	0.9727	3.8478	4.6376	0.1693	0.9724	3.8686	4.6605	0.1702	0.9726	3.8555	4.6480	0.1696	0.9723	3.8764	4.6651	0.1705
72	0.9823	3.0501	3.7369	0.1342	0.9821	3.0594	3.7549	0.1346	0.9824	3.0324	3.7240	0.1334	0.9820	3.0729	3.7609	0.1352

A more marked reduction in performance (Table 2) is observed passing from a lag time of 3 h (Model I— $R^2 = 0.9949$  —  $RAE = 0.0697$ , Model IV— $R^2 = 0.9947$  —  $RAE = 0.0717$ ) to 6 h (Model I— $R^2 = 0.9737$  —  $RAE = 0.1639$ , Model IV— $R^2 = 0.9729$  —  $RAE = 0.1662$ ). This result may essentially be attributed to the characteristics of the astronomical tide, which is basically semidiurnal, with two maximum heights and two minimum heights within 24 h. This involves the autocorrelation function [46] of the tide level time series showing positive peaks every 12 h starting from a lag time  $t_a = 12$  h and negative peaks every 12 h starting from  $t_a = 6$  h (Figure 3). For lag times corresponding to negative peaks of autocorrelation, the predictive ability of the model tends to decrease. However, the evaluation metrics show that results are still accurate (Model IV— $R^2 = 0.9729$  —  $RAE = 0.1662$ ).

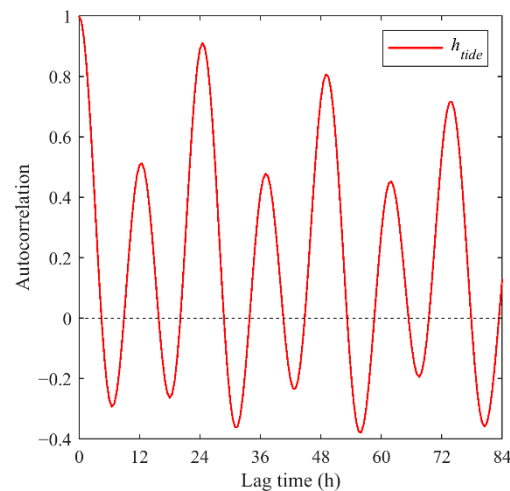


**Figure 3.** Autocorrelation function of the tide level time series measured at Punta della Salute.

After  $t_a = 6$  h, the predictions returned to slightly improve with the best performances achieved for a lag time corresponding to the positive autocorrelation peaks, showing evaluation metrics that settled on good values even for  $t_a$  equal to 72 h. Figure 4 shows the tide prediction with Model I and four different lag times for the high-tide event that took place between 23 and 26 December 2021. The three warning levels are also reported, with *high tide* between 80 cm and 110 cm, *very high tide* between 110 cm and 140 cm, and *exceptional tide* above 140 cm. It should be noted that at 110 cm, 12% of the Venice historical center and Giudecca is underwater and at 140 cm 59% is underwater [47]. During the shown period, two *exceptional tide* events were measured, respectively on 23 and 25 December, interspersed with a *very high tide*, measured on 24 December. For the first *exceptional tide*, the NARX modeling led to a slight overestimation of the tide level of 0.6 cm for  $t_a = 1$  h (Figure 4a) and to an underestimation of 3.28 cm, 6.03 cm and 2.40 cm computed respectively for  $t_a$  equal to 6 h (Figure 4b), 24 h (Figure 4c) and 72 h (Figure 4d). For the second *exceptional tide*, overestimations of 0.18 cm and 1.80 cm were computed for  $t_a$  equal to 1 h (Figure 4a) and 6 h (Figure 4b), while underestimations equal to 4.59 cm and 0.23 cm were computed for  $t_a$  equal to 24 h (Figure 4c) and 72 h (Figure 4d). For the intermediate *very high tide*, an overestimation of the tide level equal to 1.00 cm was computed for  $t_a = 6$  h, while underestimations of 0.48 cm, 7.45 cm and 3.70 cm were computed for  $t_a = 72$  h.

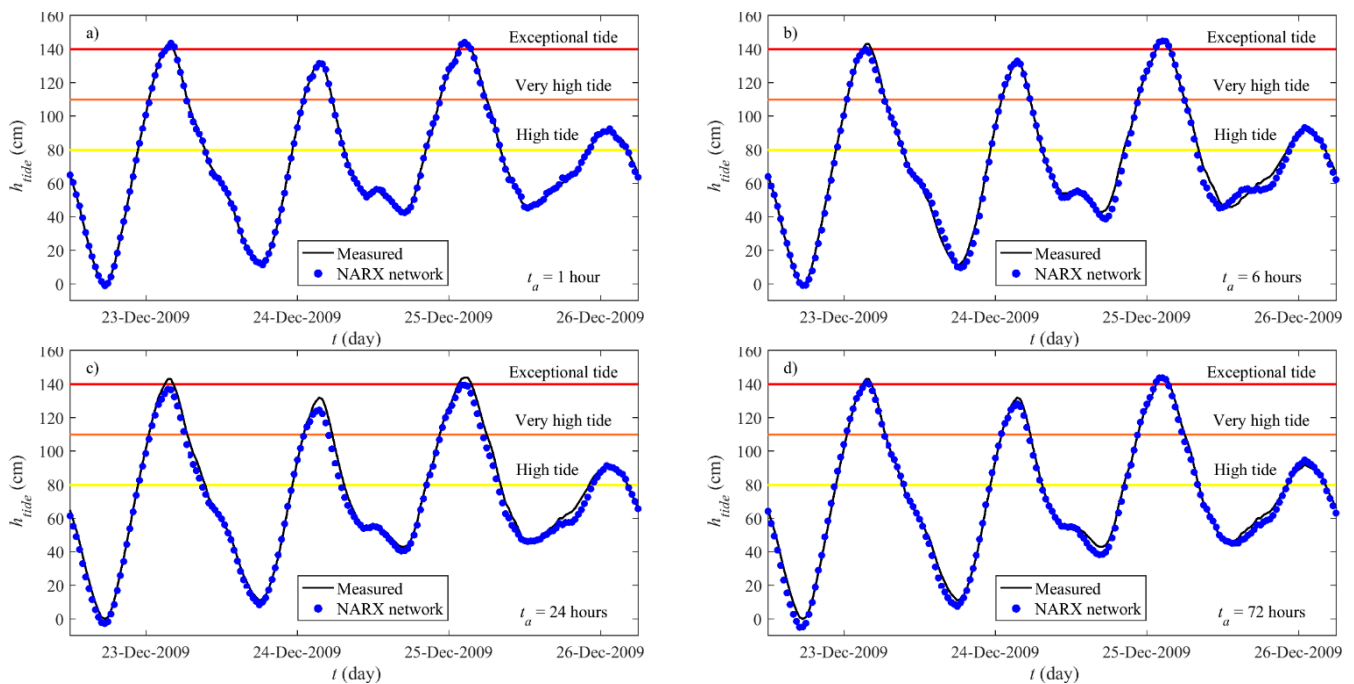


**Figure 4.** Tide prediction for Punta della Salute—Training and testing stage for Model I:  $t_a = 1$  h (a);  $t_a = 6$  h (b);  $t_a = 24$  h (c);  $t_a = 72$  h (d).

Overall, regardless of the lag time, the NARX network is able to predict both the positive and negative peaks, including the *exceptional tide*, with the best performance observed for the lowest  $t_a$  equal to 1 h. Contrary to what was expected, tide predictions obtained for  $t_a = 72$  h outperformed the ones achieved for  $t_a = 24$  h, confirming the ability of NARX models in long-term predictions.

In addition, the training and testing stage was not significantly affected by the additional input parameters: the four models showed very similar values of the evaluation metrics. This obviously does not mean that the weather parameters have little influence on high waters: the fundamental influence of the weather parameters is taken into account by means of the lagged values of the tide height.

### 3.2. Venice Lagoon Analysis

The model developed using Punta della Salute data was then validated for the entire Venetian Lagoon. Before carrying out the validation, the propagation of the tide in the lagoon was studied using an unconventional approach based on the cross-correlation function  $XCF$  between the tide level in Piattaforma CNR and the tide level in the different tide-gauge stations. The calculations were carried out with reference to the year 2009. After calculating the cross-correlation between the tide time series (Figure 5), the tide lag time  $t_{d,c}$  was evaluated as the time that maximizes the cross-correlation function:

$$t_{d,c} = \max(XCF) = \max \left( \int_0^s h_{tide, Piattaforma\ CNR}(t) h_{tide, i}(t + \tau) d\tau \right) \quad (13)$$

where  $s$  is the size of the time series and  $\tau$  is the delay [48]. Lag times are represented in Figure 6 and reported, with the peaks of cross-correlation, in Table 3. Peaks get high values, greater than 0.95 for all tide gauge stations, showing a high similarity between the tide levels inside and outside the lagoon. The lowest values are observed in correspondence with the most distant stations and with shallower bottoms. However, the propagation of the tide occurs gradually, with  $t_{d,c}$  that passes from values lower than or equal to 0.5 h near the lagoon inlets (values below 0.5 h cannot be detected due to data temporal resolution),

e.g., Malamocco Diga Nord (Figure 5a), Lido Diga Nord (Figure 5b), and Lido Diga Sud (Figure 5c), up to values over 3 h in the peripheral areas of the lagoon, e.g., Grassabò ( $t_{d,c} = 3.5$  h, Figure 5c). Instead, the central areas of the lagoon are characterized by intermediate lag times. As an example, for Punta della Salute (Figure 5b) and Treporti (Figure 5c),  $t_{d,c}$  equal to 1.5 h and 2.0 h was respectively estimated. It should be noted that the tide gauges of Valle Averteo (Figure 5a) and Marghera (Figure 5b), despite a relevant distance from the Malamocco and Lido inlets, highlight a  $t_{d,c} = 2$  h, equal to those computed in the central area of the Lagoon. This could be explained by the less-sheltered position of these tide gauges in comparison with other peripheral tide gauges, such as Grassabò (Figure 5c) and Cavallino Centro ( $t_{d,c} = 4.0$  h). These results are in agreement with Ferla et al. [49].

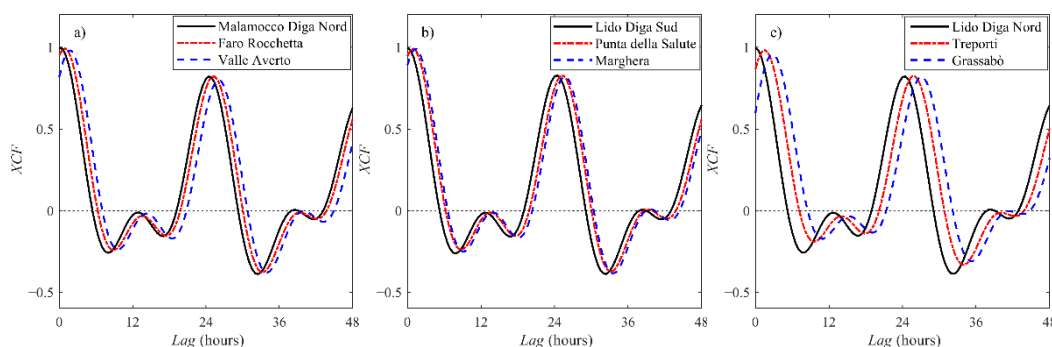


**Figure 5.** Cross-correlation function between the tide level in Piattaforma CNR and tide level in: Malamocco Diga Nord, Faro Rocchetta and Valle Averteo (a); Lido Diga Nord, Punta della Salute and Valle Averteo (b); Lido Diga Sud, Treporti and Grassabò (c).

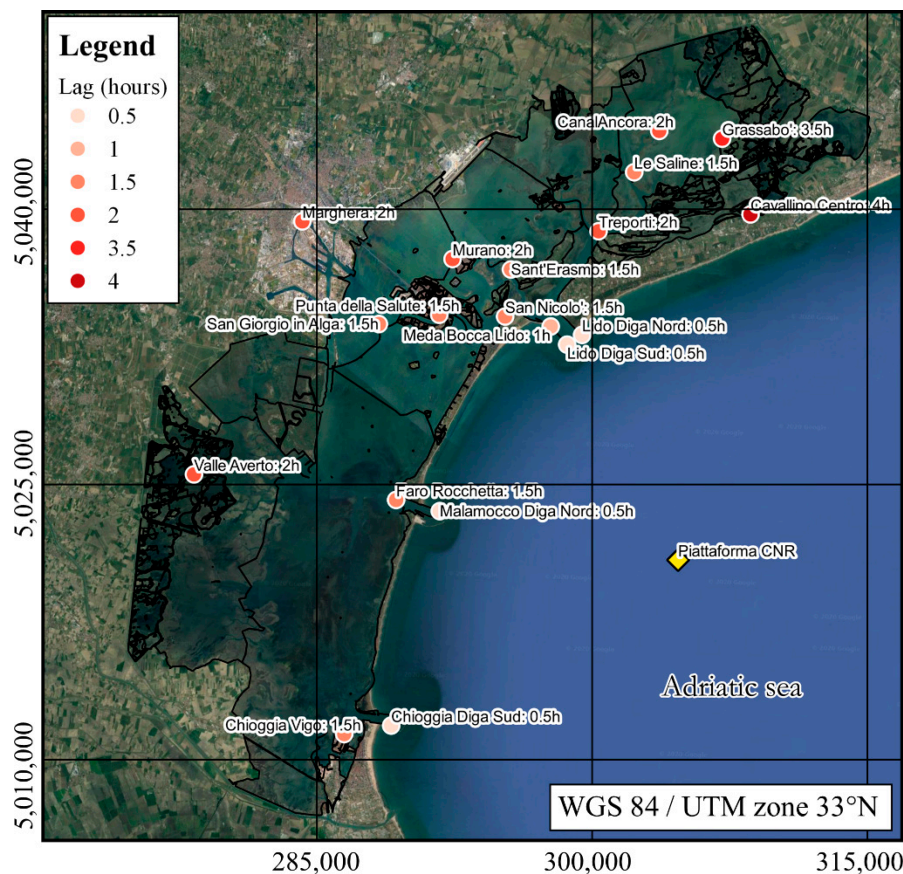


**Figure 6.** Scattered map of the lag times  $t_{d,c}$ .

**Table 3.** Lag times and cross-correlation peaks.

Tide Gauge	Lag Times (Hours)	Cross-Correlation Peaks
Canal Ancora	2.0	0.9814
Cavallino Centro	4.0	0.9548
Chioggia Diga Sud	0.5	0.9977
Chioggia Vigo	1.5	0.9913
Faro Rocchetta	1.5	0.9933
Grassabò	3.5	0.9546
Le Saline	1.5	0.9933
Lido Diga Nord	0.5	0.9969
Lido Diga Sud	0.5	0.9965
Malamocco Diga Nord	0.5	0.9946
Marghera	2.0	0.9883
Meda Bocca Lido	1.0	0.9914
Murano	2.0	0.9881
Punta della Salute	1.5	0.9915
San Giorgio in Alga	1.5	0.9882
San Nicolò	1.5	0.9912
Sant'Erasmus	1.5	0.9899
Treporti	2.0	0.9826
Valle Averte	2.0	0.9797

The  $R^2$  and  $RAE$  scattered maps for tide prediction in all the 19 tide gauge stations are shown in Figure 7, for Model I and  $t_a$  equal to 1 h and for Model IV and  $t_a$  equal to 72 h. The NARX modeling was accurate for all locations, with  $R^2$  values that never drop below 0.91 and  $RAE$  values always lower than 0.3 for  $t_a = 72$  h. Furthermore, for  $t_a = 1$  h,  $R^2$  was always higher than 0.99 and  $RAE$  was lower than 0.085 for all tide-gauge stations.

An overview of the results is given in Table 4, with a statistical analysis that consists of the evaluation of the minimum, maximum, mean, and standard deviation values of the evaluation metrics computed considering all tide-gauge stations and lag times. The best performances were observed for Model II, which exhibit mean  $R^2$  and  $RAE$  equal to 0.9298 and 0.2446, respectively. Model I shows slightly lower performances, with mean  $R^2 = 0.9286$  and mean  $RAE = 0.2472$ . This demonstrates the low impact of the barometric pressure on the tide-level prediction. Model III is outperformed by Models I and II (mean  $R^2 = 0.9263$  and mean  $RAE = 0.2494$ ); this further highlights that wind speed and direction have a greater impact on tide prediction in comparison with barometric pressure. However, tide predictions were very accurate regardless of whether weather parameters were considered as input variables, with Model IV that is characterized by the least accurate outcomes, but still close to the results of the other three models (mean  $R^2 = 0.9257$  and mean  $RAE = 0.2476$ ), confirming the great forecasting capability of the NARX network. For all 19 tide-gauge stations, an  $R^2$  greater than 0.7 was calculated, which is usually considered the minimum value for a proper prediction [50].

**Table 4.** Venice Lagoon prediction performance.

	<b>Model I</b>				<b>Model II</b>				<b>Model III</b>				<b>Model IV</b>			
	$R^2$	<i>MAE</i> (cm)	<i>RMSE</i> (cm)	<i>RAE</i>	$R^2$	<i>MAE</i> (cm)	<i>RMSE</i> (cm)	<i>RAE</i>	$R^2$	<i>MAE</i> (cm)	<i>RMSE</i> (cm)	<i>RAE</i>	$R^2$	<i>MAE</i> (cm)	<i>RMSE</i> (cm)	<i>RAE</i>
Min	0.7618	1.0035	1.3026	0.0483	0.7688	1.0067	1.3062	0.0485	0.7760	1.0129	1.3130	0.0488	0.7421	1.0079	1.3075	0.0486
Max	0.9974	11.087	13.7120	0.4895	0.9974	10.791	13.5100	0.4764	0.9973	10.679	13.481	0.4714	0.9974	11.389	14.255	0.5036
Mean	0.9286	5.2353	6.4746	0.2472	0.9298	5.1817	6.4370	0.2446	0.9263	5.2832	6.5582	0.2494	0.9257	5.2467	6.5586	0.2476
Std Dev	0.0499	2.2295	2.7109	0.1041	0.0492	2.1582	2.6578	0.1005	0.0525	2.2812	2.8037	0.1063	0.0576	2.3025	2.8918	0.1071

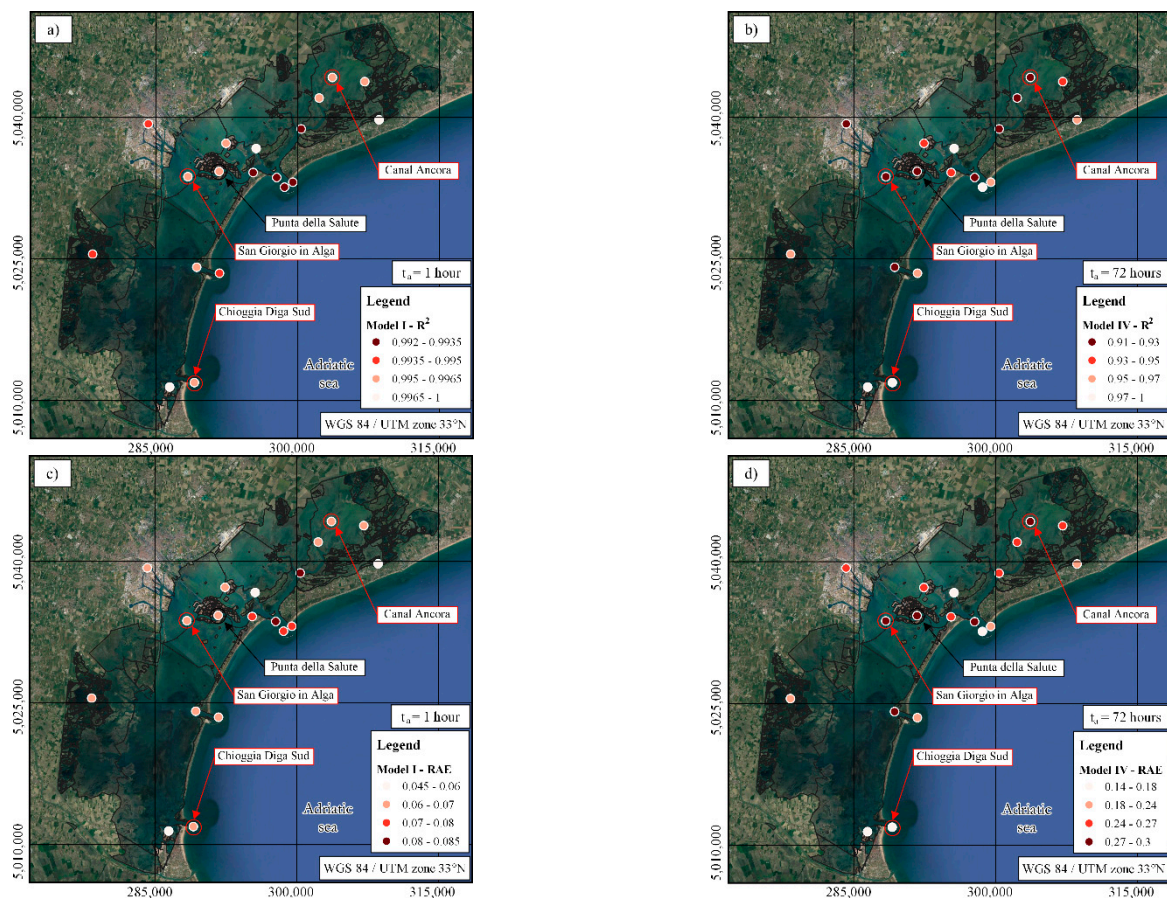


**Figure 7.**  $R^2$  and RAE scattered maps: Model I— $R^2$  and  $t_a = 1$  h (a); Model IV— $R^2$  and  $t_a = 72$  h (b); Model I—RAE and  $t_a = 1$  h (c); Model IV—RAE and  $t_a = 72$  h (d).

### 3.3. High Tide Analysis

The most interesting issue in tide modeling is represented by the prediction of high tides. In the training and testing stage, the NARX network proved to be able to predict even an *exceptional tide* for Punta della Salute. In this section, the results relating to the high-tide predictions for three tide-gauge stations located in different points of the Venice Lagoon are described and discussed. Compared to the training and testing stage, a shorter simulation period, equal to one year, was considered.

The first tide gauge was Chioggia Diga Sud located in proximity of the Chioggia Inlet, in the south of the Venice Lagoon. In the period between 10 and 12 February 2014 in this station, a *very high tide* of 130 cm was measured, followed by a *high tide* of 95 cm (Figure 8a). The tide level reached at Chioggia Inlet was, however, higher than those recorded in the same period at the Lido inlet and in the Venice historical center, with peaks of 98 cm and 108 cm measured, respectively, in the stations of Treporti and Punta della Salute. NARX modeling, with Model IV and  $t_a = 72$  h, provided accurate forecasting of both high tide measurements for Chioggia Diga Sud, with an underestimation of the *very high tide* event of only 1.90 cm and to an underestimation of the *high tide* event of 2.85 cm.

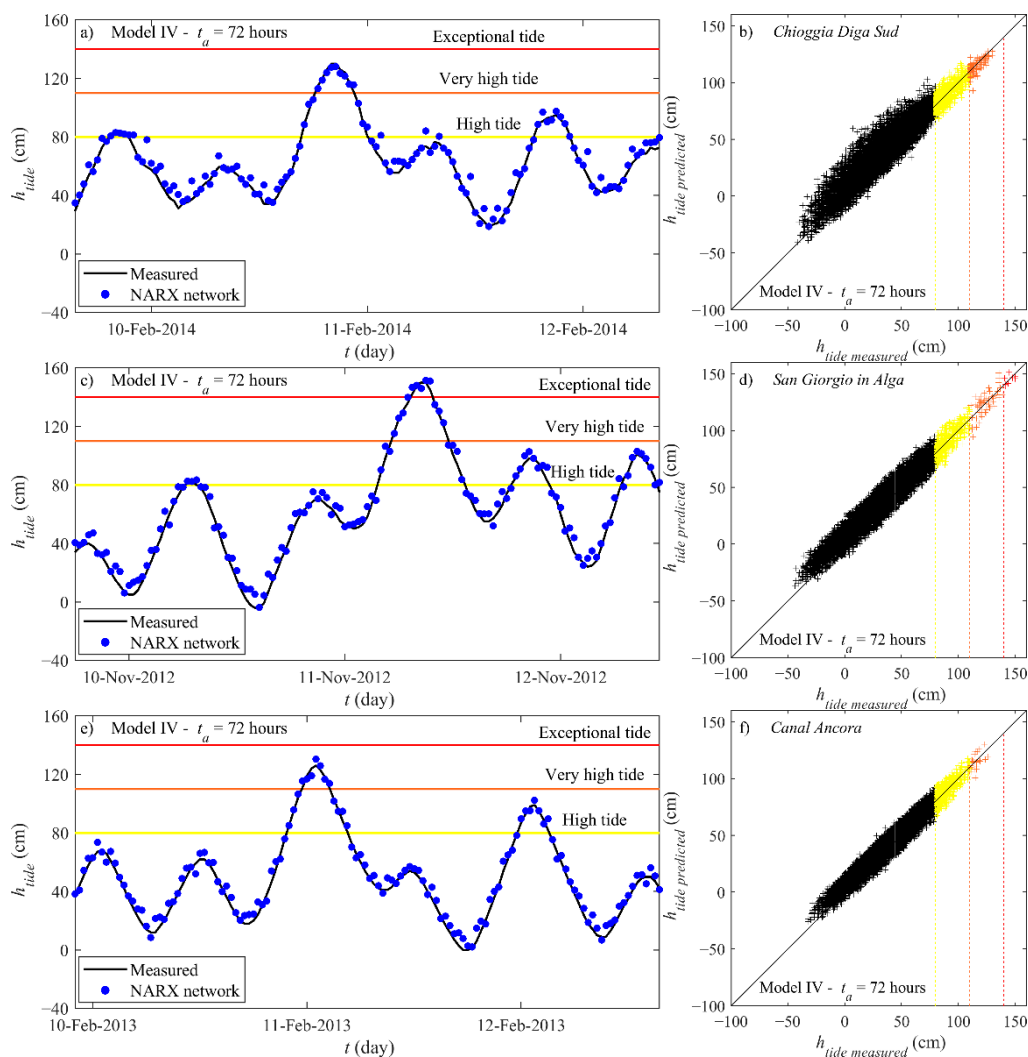


**Figure 8.** High tide prediction (Model IV— $t_a = 72$  h). On the **left**: Chioggia Diga Sud—time series in the period between 10 and 12 February 2014 (a); San Giorgio in Alga—time series in the period between 10 and 12 November 2012 (c); Canal Ancora—time series in the period between 10 and 12 February 2013 (e). On the **right**, predicted versus measured values for the validation period for: Chioggia Diga Sud (b); San Giorgio in Alga (d); Canal Ancora (e).

The second tide gauge was San Giorgio in Alga, located in a homonymous small island in the middle of the lagoon, close to the Giudecca island and historical center. An *exceptional tide* height of 150 cm was measured at this station on 11 November 2012 and two *high tides*, with heights between 80 cm and 110 cm, were measured until the following day (Figure 8c). In the nearby station of Punta della Salute, a similar *exceptional tide* height of 148 cm was measured at the same time. For the *exceptional tide* measured in San Giorgio in Alga, NARX modeling led to an overestimation of 1.37 cm computed, while for the subsequent two *high tides*, higher overestimations were observed, respectively equal to 4.75 cm and 1.81 cm.

The third was Canal Ancora, located in the north of the lagoon. For this tide gauge, the most significant peak measured in 2013 was equal to 126 cm, which corresponds to a *very high tide* (Figure 8e). It should be noted that, in the same day, 11 February 2013, in Punta della Salute an *exceptional tide* of 142 cm was recorded (Figure 4). The difference of 16 cm between Punta della Salute and Canal Ancora was caused by the propagation of the flood event, which initially affected the central part of the lagoon and then reached the peripheral areas, located at a greater distance from the three inlets, and by the configuration of the lagoon seabed. NARX modeling provided good predictions also for

Canal Ancora, with limited overestimations of the tide level equal to 4.32 cm and 3.17 cm for the *very high tide* and *high tide*, respectively.

Overall, the position of the three tide gauges with respect to the weather station, more or less distant from the Lagoon inlets, did not affect the accuracy of the forecast. The tide prediction performed with the simplest model, Model IV, and the highest lag time, equal to 72 h, confirm the ability of the NARX network to predict high tides, even in case of exceptional events. In addition, the forecasts of *exceptional tide* showed similar accuracy to that observed for *very high tides* and *high tides* events, confirming the suitability of the NARX network for the modeling of extreme events. The same accuracy was also achieved in predicting negative peaks or tides between 0 and 80 cm (Figure 8b,d,f). The best performance was obtained for Chioggia Diga Sud with  $R^2 = 0.9764$  and  $RAE = 0.1536$ . Slightly lower but still very accurate predictions were achieved for Canal Ancora ( $R^2 = 0.92613$  and  $RAE = 0.2709$ ) and for San Giorgio in Alga ( $R^2 = 0.9141$  and  $RAE = 0.2906$ ).

Further confirmation of the results accuracy obtained through Model IV is shown in Figure 9, which reports a notched box plots representation of the *Residuals*, expressed as the difference between measured and predicted values, for  $h_{tide} > 80$  cm, as the lag time increases. It should be noted that positive *Residuals* involve an underestimation of positive tide peaks that correspond to high tides, while negative *Residuals* involve an overestimation of negative tide peaks that correspond to low tides. For the three stations, whiskers ranged between  $-4$  cm and  $6$  cm and medians between  $-0.5$  cm and  $2.5$  cm. Exceptions to these results were observed for  $t_a = 6$  h where there is a relevant underestimation of high tides with whiskers ranged between  $5$  cm and  $20$  cm and the medians between  $9$  cm and  $13$  cm. These discrepancies may be explained with the autocorrelation analysis reported in Section 3.2. The best performances were achieved for  $t_a$  equal to 1 h. However, for  $t_a$  equal to 72 h, the outliers (red crosses in Figure 9) were a small percentage: 4.62% for Chioggia Diga Sud, 3.04% for San Giorgio in Alga, and 4.82% for Canal Ancora.

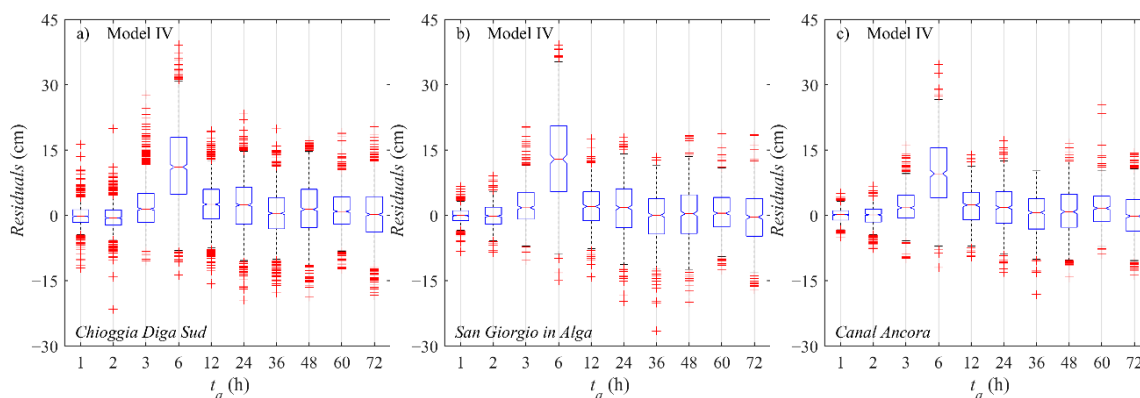


**Figure 9.** Tide prediction—Model IV, residuals box plots for  $h_{tide} > 80$  cm, expressed as the lag time  $t_a$  increases, for: Chioggia Diga Sud (a); San Giorgio in Alga (b); Canal Ancora (c). The lower end of each box plot denotes the 1st quartile (25th percentile); the upper end denotes the 3rd quartile (75th percentile). The “notch” represents the 95% confidence interval of the median.

Good results were also achieved without including the weather data related to the wind and barometric pressure, with Model IV capable of providing accurate predictions. This aspect probably represents one of the most interesting novel results of this study. Moreover, this made it possible to extend the analysis through Model IV to a longer period, from January 2009 to December 2018, allowing the validation of the model on a wider range of events, using the tide-level dataset measured in Punta della Salute, while the trained NARX-based model is the same developed and described in Section 3.1.

Figure 10 shows some results of this modeling, obtained for a  $t_a = 72$  h, focusing on the highest tide measured in Punta della Salute in the period 2009–2018, equal to 154 cm. As can be seen from the residuals, properly divided in order to take into account the

values of *high tide*, *very high tide* and *exceptional tide*, the model provided predictions with small underestimation and overestimations. For the *exceptional tide*, equal to 154 cm, the level is underestimated at about 6.08 cm. The second *exceptional tide*, which was observed after few hours, shows an even lower underestimation, equal to 2.95 cm. For  $h_{tide} < 80$  cm and  $80 \text{ cm} < h_{tide} < 110$  cm, some overestimations of the tide level are also observed, with values lower than 5.4 cm. A maximum underestimation of 4.15 cm was evaluated for a high tide event, on 31 October 2018. In any case, forecast errors can be significantly reduced with the progressive use of NARX-based models characterized by gradually decreasing  $t_a$ .

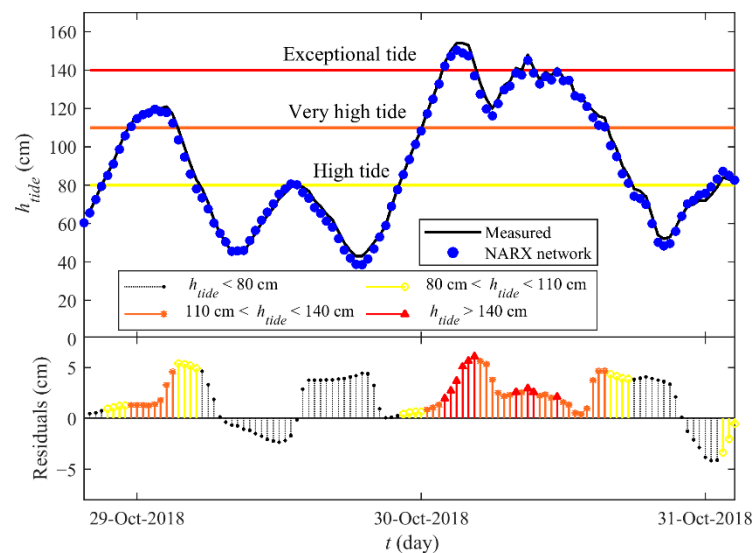


**Figure 10.** Exceptional high tide in Punta della Salute (event of 28–31 October 2018): comparison between measured time series and predicted values with Model IV and  $t_a = 72$  h (**upper chart**), *Residuals* (**lower chart**).

The results obtained also lend themselves to an interesting interpretation from the physical point of view. The possibility of predicting high waters with excellent accuracy regardless of weather-forcing data, even a few days in advance, shows that the complex system represented by the Venice lagoon is characterized by considerable “inertia”. In particular, when exceptional high waters occur, meteorological factors begin to influence the phenomenon a few days earlier. The effects persist for some days, during which there are some significant peaks of high tide. Furthermore, the study of the cross-correlation function between the oscillations in the different points of the lagoon allow obtaining relevant information on the propagation of the tide without having to conduct a hydrodynamic study and without having to know in detail the configuration of the lagoon itself. Ultimately, the proposed models make it possible to obtain accurate forecasts for a large area on the basis of limited information relating to two or even a single measurement station: this aspect also distinguishes them from commonly used forecasting models, which instead require measurements of the input in a large area.

#### 4. Conclusions

This study assessed the ability of the Nonlinear Autoregressive Exogenous neural network to develop forecasting models of the tide level in the Venice Lagoon. Four models were built, including both the lagged values of the tide level and astronomical tide as input values. In each model, different combinations of additional input values were considered in order to take into account the meteorological parameters related to wind features and barometric pressure.

Very accurate tide predictions were achieved regardless of whether the meteorological parameters were considered as input parameters. The ability to forecast even exceptionally high tides makes the NARX neural networks a reliable tool for predicting tide-level

fluctuation. In addition, the modeling was not particularly affected by lag-time increase, with a satisfactory performance achieved also for a  $t_a$  equal to 72 h: this demonstrates the great capability of NARX networks to predict high waters with a forecasting horizon of several days.

Therefore, NARX modeling could represent a reliable approach for the management of the MOSE, ensuring an adequate time interval for the activation of the barriers. This would allow a reduction of the disaster risk for the city of Venice (Goal 11 of the 2030 Agenda for Sustainable Development), contrasting the effects of climate change that will lead to a rise in the average sea level (Goal 13) and, at the same time, protecting the biodiversity and ecosystem of the Venice Lagoon (Goal 15).

However, even though meteorological parameters may not be included in the model input data, their significant influence is implicitly expressed by including previously observed tidal height values. In addition, in order to provide accurate forecasting of the tide level, it is recommended to consider the astronomical tide as exogenous input. Furthermore, a time-series length of at least 12 months, with different extreme events during the time interval, is necessary for a proper training of the NARX network.

The good results obtained for the Venice Lagoon recommend the use of the NARX network for tide prediction in coastal areas affected by problems related to high tides. A proper evaluation of the tide level is a key factor for the safeguard of the economic, social, and cultural heritage of these places. In addition, the proposed model could be a support tool for the decisions regarding the timely activation of the MOSE in the Venice Lagoon, and of similar systems in other places around the world.

**Author Contributions:** Conceptualization, F.G.; methodology, F.D.N. and F.G.; software, F.D.N.; validation, F.G. and R.G.; formal analysis, F.G. and F.D.N.; investigation, F.D.N., F.G., R.G. and G.d.M.; resources, F.G.; data curation, F.D.N. and F.G.; writing—original draft preparation, F.D.N.; writing—review and editing, F.G., R.G. and G.d.M.; supervision, F.G.; project administration, G.d.M. All authors have read and agreed to the published version of the manuscript.

**Funding:** This research received no external funding.

**Institutional Review Board Statement:** Not applicable.

**Informed Consent Statement:** Not applicable.

**Data Availability Statement:** The data are freely available online on the website [https://www.venezia.isprambiente.it/index.php?folder\\_id=20&lang\\_id=2](https://www.venezia.isprambiente.it/index.php?folder_id=20&lang_id=2) (accessed on 23 April 2021).

**Conflicts of Interest:** The authors declare no conflict of interest.

## References

- Umgiesser, G. The impact of operating the mobile barriers in Venice (MOSE) under climate change. *J. Nat. Conserv.* **2020**, *54*. [[CrossRef](#)]
- Bras, R.L.; Harleman, D.R.F.; Rinaldo, A.; Rizzoli, P. Rescuing Venice from a watery grave. *Science* **2001**, *291*, 2315–2316. [[CrossRef](#)]
- Tosi, L.; Teatini, P.; Strozzi, T. Natural versus anthropogenic subsidence of Venice. *Sci. Rep.* **2013**, *3*, 1–9. [[CrossRef](#)]
- Trincardi, F.; Barbanti, A.; Bastianini, M.; Benetazzo, A.; Cavaleri, L.; Chiggiato, J.; Papa, A.; Pomaro, A.; Sclavo, M.; Tosi, L.; et al. The 1966 Flooding of Venice: What Time Taught Us for the Future. *Oceanography* **2016**, *29*, 178–186. [[CrossRef](#)]
- Comune di Venezia. Centro Previsioni e Segnalazioni Maree—Dati e statistiche—Archivio storico: Livello di marea a Venezia. 2020. Available online: <https://www.comune.venezia.it/node/6214> (accessed on 23 April 2021).
- Reimann, L.; Vafeidis, A.; Brown, S.; Hinkel, J.; Tol, R. Mediterranean UNESCO World Heritage at risk from coastal flooding and erosion due to sea-level rise. *Nat. Commun.* **2018**, *9*. [[CrossRef](#)]
- Tosoni, A.; Canestrelli, P. Il modello stocastico per la previsione di marea a Venezia. *Atti Ist. Veneto Sci. Lett. Arti* **2011**, *169*, 2010–2011.
- Massalin, A.; Zampato, L.; Papa, A.; Canestrelli, P. Data monitoring and sea level forecasting in the Venice Lagoon: The ICPSM's activity. *Boll. Geofis. Teor. Appl.* **2007**, *48*, 241–257.
- Lovato, T.; Androsov, A.; Romanenkov, D.; Rubino, A. The tidal and wind induced hydrodynamics of the composite system Adriatic Sea/Lagoon of Venice. *Cont. Shelf Res.* **2010**, *30*, 692–706. [[CrossRef](#)]
- Umgiesser, G.; Canu, D.M.; Cucco, A. A finite element model for the Venice Lagoon. Development, set up, calibration and validation. *J. Mar. Syst.* **2004**, *51*, 123–145. [[CrossRef](#)]

11. Lionello, P.; Sanna, A.; Elvini, E.; Mufato, R. A data assimilation procedure for operational prediction of storm surge in the northern Adriatic Sea. *Cont. Shelf Res.* **2006**, *26*, 539–553. [[CrossRef](#)]
12. Mel, R.; Viero, D.P.; Carniello, L.; Defina, A.; D'Alpaos, L. Simplified methods for real-time prediction of storm surge uncertainty: The city of Venice case study. *Adv. Water Resour.* **2014**, *71*, 177–185. [[CrossRef](#)]
13. Canestrelli, E.; Canestrelli, P.; Corazza, M.; Filippone, M.; Giove, S.; Masulli, F. Local Learning of Tide Level Time Series using a Fuzzy Approach. In Proceedings of the IEEE International Joint Conference on Neural Networks, Orlando, FL, USA, 12–17 August 2007; pp. 1813–1818.
14. Parise, F.; Picci, G. Identification of High Tide Models in the Venetian Lagoon: Variable Selection and G-LASSO. *Int. Fed. Autom. Control* **2014**, *19*. [[CrossRef](#)]
15. Wei, H.L.; Billings, S.A. An efficient nonlinear cardinal B-spline model for high tide forecasts at the Venice Lagoon. *Nonlinear Process. Geophys.* **2006**, *13*, 577–584. [[CrossRef](#)]
16. Chau, K.W.; Wu, C.; Li, Y.S. Comparison of Several Flood Forecasting Models in Yangtze River. *J. Hydrol. Eng.* **2005**, *10*, 485–491. [[CrossRef](#)]
17. Kişi, Ö. Streamflow forecasting using different artificial neural network algorithms. *J. Hydrol. Eng.* **2007**, *12*, 532–539. [[CrossRef](#)]
18. Tapoglou, E.; Karatzas, G.P.; Trichakis, I.C.; Varouchakis, E.A. A spatio-temporal hybrid neural network-Kriging model for groundwater level simulation. *J. Hydrol.* **2014**, *519*, 3193–3203. [[CrossRef](#)]
19. Najafzadeh, M.; Etemad Shahidi, A.; Lim, S.Y. Scour Prediction in Long Contractions Using ANFIS and SVM. *Ocean Eng.* **2016**, *111*, 128–135. [[CrossRef](#)]
20. Khan, N.; Sachindra, D.A.; Shahid, S.; Ahmed, K.; Shiru, M.S.; Nawaz, N. Prediction of droughts over Pakistan using machine learning algorithms. *Adv. Water Resour.* **2020**, *139*, 103562. [[CrossRef](#)]
21. Phan, T.T.H.; Nguyen, X.H. Combining statistical machine learning models with ARIMA for water level forecasting: The case of the Red river. *Adv. Water Resour.* **2020**, *142*, 103656. [[CrossRef](#)]
22. Granata, F.; Gargano, R.; de Marinis, G. Artificial intelligence based approaches to evaluate actual evapotranspiration in wetlands. *Sci. Total Environ.* **2020**, *703*, 135653. [[CrossRef](#)]
23. Zaldivar, J.M.; Gutiérrez, E.; Galván, I.M.; Strozzi, F.; Tomasin, A. Forecasting high waters at Venice Lagoon using chaotic time series analysis and nonlinear neural networks. *J. Hydroinform.* **2000**, *2*, 61–84. [[CrossRef](#)]
24. Rakshith, S.; Dwarakish, G.S.; Natesan, U. Tidal-Level forecasting using Artificial Neural Networks along the West Cost of India. *J. Jpn. Soc. Civ. Eng.* **2014**, *2*, 176–187.
25. Riazi, A. Accurate tide level estimation: A deep learning approach. *Ocean Eng.* **2020**, *198*. [[CrossRef](#)]
26. Todini, E. Hydrological catchment modelling: Past, present and future. *Hydrol. Earth Syst. Sci.* **2007**, *11*, 468–482. [[CrossRef](#)]
27. Abe, S. *Support Vector Machines for Pattern Classification*; Springer: Dordrecht, The Netherlands, 2010; p. 473.
28. Solomatine, D.P.; Ostfeld, A. Data-driven modelling: Some past experiences and new approaches. *J. Hydroinform.* **2008**, *10*, 3–22. [[CrossRef](#)]
29. Varouchakis, E.A.; Spanoudaki, K.; Hristopulos, D.T.; Karatzas, G.P.; Corzo, G. Stochastic Modeling of Aquifer Level Temporal Fluctuations Based on the Conceptual Basis of the Soil-Water Balance Equation. *Soil Sci.* **2016**, *181*, 224–231. [[CrossRef](#)]
30. Varouchakis, E.A. Modeling of temporal groundwater level variations based on a kalman filter adaptation algorithm with exogenous inputs. *J. Hydroinform.* **2017**, *19*, 191–206. [[CrossRef](#)]
31. Alsumaiei, A.A. A Nonlinear Autoregressive Modeling Approach for Forecasting Groundwater Level Fluctuation in Urban Aquifers. *Water* **2020**, *12*, 820. [[CrossRef](#)]
32. Berbić, J.; Ocvirk, E.; Carevic, D.; Loncar, G. Application of neural networks and support vector machine for significant wave height prediction. *Oceanologia* **2017**, *59*, 331–349. [[CrossRef](#)]
33. Di Nunno, F.; Granata, F. Groundwater level prediction in Apulia region (Southern Italy) using NARX neural network. *Environ. Res.* **2020**, *190*, 110062. [[CrossRef](#)]
34. Tahmasebi, P.; Kamrava, S.; Bai, T.; Sahimi, M. Machine learning in geo- and environmental sciences: From small to large scale. *Adv. Water Resour.* **2020**, *142*. [[CrossRef](#)]
35. Semprucci, F.; Balsamo, M.; Sandulli, R. Assessment of the ecological quality (EcoQ) of the Venice lagoon using the structure and biodiversity of the meiofaunal assemblages. *Ecol. Indic.* **2016**, *67*, 451–457. [[CrossRef](#)]
36. Pivato, M.; Carniello, L.; Gardner, J.; Silvestri, S.; Marani, M. Water and sediment temperature dynamics in shallow tidal environments: The role of the heat flux at the sediment-water interface. *Adv. Water Resour.* **2018**, *113*, 126–140. [[CrossRef](#)]
37. Comune di Venezia. Centro Previsioni e Segnalazioni Maree-La Marea-La Marea Astronomica. 2020. Available online: <https://www.comune.venezia.it/it/content/la-marea-astronomica> (accessed on 23 April 2021).
38. ASCE Task Committee on Application of Artificial Neural Networks in Hydrology. Artificial neural networks in hydrology. I: Preliminary concepts. *J. Hydrol. Eng.* **2000**, *5*, 115–123. [[CrossRef](#)]
39. Guzman, S.M.; Paz, J.O.; Tagert, M.L.M. The Use of NARX Neural Networks to Forecast Daily Groundwater Levels. *Water Resour. Manag.* **2017**, *31*, 1591–1603. [[CrossRef](#)]
40. Desouky, M.M.A.; Abdelkhalik, O. Wave prediction using wave rider position measurements and NARX network in wave energy conversion. *Appl. Ocean Res.* **2019**, *82*, 10–21. [[CrossRef](#)]
41. MathWorks. *MATLAB Deep Learning Toolbox Release 2020a*; MathWorks: Natick, MA, USA, 2020.

42. Di Nunno, F.; Granata, F.; Gargano, R.; de Marinis, G. Forecasting of Extreme Storm Tide Events Using NARX Neural Network-Based Models. *Atmosphere* **2021**, *12*, 512. [[CrossRef](#)]
43. MacKay, D.J.C. Bayesian Interpolation. *Neural Comput.* **1992**, *4*, 415–447. [[CrossRef](#)]
44. Foresee, F.D.; Hagan, M.T. Gauss-Newton approximation to Bayesian learning. In Proceedings of the International Conference on Neural Networks (ICNN'97), Houston, TX, USA, 12 June 1997; pp. 1930–1935. [[CrossRef](#)]
45. Bishop, C.M. *Neural Networks for Pattern Recognition*; Oxford University Press: New York, NY, USA, 1995; p. 198.
46. Box, G.E.P.; Jenkins, G.M.; Reinsel, G.C. *Time Series Analysis: Forecasting and Control*, 3rd ed.; Prentice Hall: Englewood Cliffs, NJ, USA, 1994.
47. Comune di Venezia. Centro Previsioni e Segnalazioni Maree-La Marea-Le Percentuali di Allagamento. 2020. Available online: <https://www.comune.venezia.it/it/content/le-percentuali-allagamento> (accessed on 23 April 2021).
48. Iannello, J.P. Time Delay Estimation Via Cross-Correlation in the Presence of Large Estimation Errors. *IEEE Trans. Signal Process.* **1982**, *30*, 998–1003. [[CrossRef](#)]
49. Ferla, M.; Cordella, M.; Michielli, L.; Rusconi, A. Long term variations on sea level and tidal regime in the lagoon of Venice. *Estuar. Coast. Shelf Sci.* **2007**, *75*, 214–222. [[CrossRef](#)]
50. Moore, D.S.; Notz, W.I.; Flinger, M.A. *The Basic Practice of Statistics*, 8th ed.; W.H. Freeman and Company, 41; Madison Avenue: New York, NY, USA, 2018; p. 654.